Int. J. Solids Structures Vol. 23, No. 11, pp. 1485–1503, 1987
Printed in Great Britain.

0020–7683/87 $3.00+ .00

NON-STATIONARY CREEP BEHAVIOR OF FLOATING ICE BEAMS UNDER LATERAL LOADS†

DAVID HUI‡
Department of Engineering Mechanics, Ohio State University, Columbus, OH 43210, U.S.A.

P. C. XIROUCHAKIS
Department of Ocean Engineering, Massachusetts Institute of Technology, Cambridge, MA 02139, U.S.A.

and

Y. H. CHEN
Department of Engineering Mechanics, Ohio State University, Columbus, OH 43210, U.S.A.

(*Received* 26 *May* 1986; *in revised form* 3 *December* 1986)

Abstract—The present study deals with the non-linear creep behavior of floating ice beams under lateral loads. The influence of the variability of Young's modulus across the beam thickness and time hardening in the power-type creep constitutive relation on the deflections and stresses of ice beams are considered. The resulting governing differential equation is solved using the central finite difference method while time integration is performed using Euler's integration scheme with a variable time step. Time hardening is found to increase the deflections and in general, further relax the stresses. Unlike the homogeneous beam, the stresses in a non-homogeneous beam may initially increase and then relax with time. The analysis takes into account the shift of the neutral axis of the beam as a function of time using small deflection beam theory.

1. INTRODUCTION

Floating ice sheets are often used for the transportation and storage of heavy vehicles and equipment in cold regions (e.g. Saint Lawrence River, Canada, and in Lake Lagoda near Leningrad, U.S.S.R.). The oil and gas exploration activities in the Arctic region have considerably increased the interest in the bearing capacity of floating ice covers as drilling platforms and layout of marine pipelines. The existing analytical and experimental data for the determination of the bearing capacity of laterally loaded floating ice plates have been thoroughly reviewed by Kerr (1976). Excellent summaries of the bearing capacity of ice and the associated failure criteria were presented by Michel (1978). The influence of rate of loading, temperature and brine volume of ice on its flexural strength as well as a comprehensive review of the viscoelastic properties and elastic modulus of ice were examined by Mellor (1983). A number of excellent Ph.D. theses on the bearing capacity of ice were written by Palmer (1971), Mohaghegh (1972), Nevel (1976), Murat (1978a, b) and Hamza (1981). Interesting papers on the above subject can be found in annual conferences (such as OMAE edited by Lunardini (1984), POAC edited by Jumppanen (1983), IAHR edited by Carstens (1984) and Offshore Technology Conference at Houston). A number of comprehensive reports were written by Panfilov (1960), Weeks and Assur (1966), Nevel (1976), Vaudrey (1977) and Lainey (1981), among others. Thus, there exists a very large number of publications on the mechanical behavior of floating ice covers.

Linear (creep strain rate proportional to the applied stress) viscoelastic constitutive relations for floating ice plate deformations were employed by Vaudray and Katona (1975), Vaudray (1977), Novel (1976), Fransson (1985) and Hui (1986). Finite element analyses of the non-linear flexural creep behavior of floating ice plates have been reported by Tinawi and Murat (1978), Swamidas *et al.* (1978), Masterson and Strandberg (1979), Hamza and Muggeridge (1982), Murat and Degrange (1983) and Tinawi and Gagnon (1984).

† Presented at the U.S. National Congress of Applied Mechanics, University of Texas at Austin, 16–20 June 1986.

‡ Now Associate Professor, University of New Orleans, Department of Mechanical Engineering, New Orleans, LA 70148, U.S.A.

However, most of the results presented are only valid for homogeneous floating ice sheets, although in actual floating ice plates, Young's modulus may vary strongly with depth (Kerr and Palmer, 1972). Further, only secondary creep solutions have been obtained in most cases and the important influences of primary creep deformations have not been considered. The study of primary creep deformation is important because in many cases of practical interest, failure (deflections exceed the freeboard) strains are small and therefore occur in the primary state of creep (Frederking and Gold, 1976; Duval *et al.*, 1981; Ponter *et al.*, 1983). This paper is the first in the literature to report the non-stationary primary creep behavior of floating ice beams, taking into account the non-homogeneity of the material and shift in the neutral axis as a function of time.

The power type constitutive relation was modified to include a time hardening exponential function suggested by Assur (1979). The exponential function and hence the strain rate has a minimum value at time $\bar{t} = \bar{t}_r$ so that $\bar{t} < \bar{t}_r$ corresponds to primary creep and $\bar{t} > \bar{t}_r$ corresponds to tertiary creep ($\bar{t}_r$ is reference time). The governing differential equation for the non-stationary creep response of a floating ice beam is derived and it is solved using a central finite difference scheme. Time integrations of the deflections and stresses are performed using Euler's integration procedure with a variable time step. As an example problem, the creep behavior of a simply supported floating ice beam subjected to a sinusoidal load (Xirouchakis, 1981) is examined. The effect of time hardening on the creep response is to increase the deflection in comparison with the secondary creep case and in general, further relax the stresses with time.

Unlike the case of a homogeneous beam (constant Young's modulus across the beam thickness), the axial stresses of a non-homogeneous beam may initially rise with time and then relax with time later on. The neutral axis (that is, the zero axial stress axis) does not change with time for a homogeneous beam and it changes with time for a non-homogeneous beam. The location of the neutral axis as well as the stress profile across the thickness are updated for each time step. Special precautions are taken on the choice of the time step to ensure correct convergence of the deflections and stresses. In passing, the shift of the neutral axis as a function of time for a beam without foundation subjected to constant end moment was examined by Findley *et al.* (1958) and summarized in his text (1976).

The time hardening constitutive relation is employed in the present analysis. However, the strain softening rule is used by a number of authors (Wang, 1983; Chen *et al.*, 1985) to predict the creep response of sea ice at low and high strain rates. The strain hardening rule was used by Hamza (1981) to predict the viscoelastic response of uniaxially loaded compression and tensile test specimens and good agreement was obtained between the numerical results and experiments (Mellor and Cole, 1982). A comparative study of the various constitutive relations which are applicable for the creep bearing capacity of ice is in progress.

2. ELASTIC RESPONSE

The elastic solution will provide the initial condition for the creep behavior of floating ice beams. The beam on a linear elastic liquid foundation (considered as a Winkler-type support) is subjected to a lateral distributed force per unit length $P(X)$ and a concentrated force P at the beam center. Further, only loads smaller than the corresponding elastic failure loads are of interest.

The potential energy of the floating ice beam subjected to lateral loads (Hui and Hansen, 1980a; Hui, 1986a, b)

$$\text{P.E.} = \int_{X=-L/2}^{L/2} [(D_1 B/2)(W_{,XX})^2 + (K_1/2)W^2 - W \cdot P(X)]\, dX - F \cdot W(X=0) \qquad (1)$$

where W is the lateral deflection, X is the axial coordinate measured from the beam center, L and B are the length and width of the beam, respectively, $K_1 = \rho g B$ and ρg is the liquid

foundation modulus. The effective flexural rigidity D_1 is defined as

$$D_1 = \int_{Z=-Z_0}^{H-Z_0} Z^2 E(Z)\, dZ \tag{2a}$$

where H is the beam thickness, Z_0 is the distance from the neutral axis to the top fiber of the beam and Z is the transverse coordinate measured from the neutral axis, positive downward. Young's modulus as a function of Z across the ice thickness is specified by (Kerr and Palmer, 1972)

$$E(Z)/E_0 = 1-(1-a)[(Z/H)+(Z_0/H)]^b. \tag{2b}$$

In the above expression, E_0 is Young's modulus of the top fiber and the Young's modulus parameters a and b are non-dimensional positive constants ($0 \leqslant a \leqslant 1$). Since the axial stress $\tilde{\sigma}_x$ is related to the bending moment M_x by

$$\tilde{\sigma}_x = (M_x/D_1)ZE(Z) \tag{2c}$$

the quantity Z_0/H which specified the location of the neutral axis is obtained by setting to zero the integral of $ZE(Z)$ through the beam thickness so that

$$z_0 = Z_0/H = \frac{(b+2a)(b+1)}{(2)(b+2)(b+a)}. \tag{3}$$

Based on the above Young's modulus profile, the non-dimensional effective flexural rigidity can be expressed in terms of a and b in the form ($z = Z/H$)

$$d_1 = 12D_1/(E_0H^3) = 12\left(\frac{(b+3a)}{3(b+3)} - \frac{(b+2a)(z_0)}{b+2} + \frac{(b+a)(z_0)^2}{b+1}\right). \tag{4}$$

The following non-dimensional quantities are introduced:

$$\begin{aligned} \lambda &= [4E_0I_0d_1/K_1]^{1/4} = (4BD_1/K_1)^{1/4} \\ w &= WH/\lambda^2, \qquad x = X/\lambda, \qquad (\ )_{,x} = (1/\lambda)(\ )_{,x} \\ p(x) &= H\lambda^2P(X)/(D_1B) = 4HP(X)/(K_1\lambda^2) \\ f &= H\lambda F/(D_1B) = 4HF/(K_1\lambda^3) \end{aligned} \tag{5}$$

where λ is the characteristic length (Hetenyi, 1946) and $I_0 = BH^3/12$. The governing differential equation can then be obtained from the potential energy with the aid of calculus of variations in the form

$$w_{,xxxx} + 4w = p(x) \tag{6}$$

where $p(x)$ is an arbitrary function of x. The associated boundary conditions at one end of the beam ($x = \pm L/(2\lambda)$) are

$$\begin{aligned} w &= 0 \quad \text{or} \quad w_{,xxx} = 0 \\ w_{,x} &= 0 \quad \text{or} \quad w_{,xx} = 0. \end{aligned} \tag{7}$$

Furthermore, assuming that the loading function $p(x)$ is symmetric with respect to the beam center, the boundary conditions at the beam center ($x = 0$) are

$$w_{,x}(x=0) = 0, \qquad w_{,xxx}(x=0) = f/2 \tag{8}$$

where the forced equilibrium requirement (that is, the reaction forces over the entire beam are equal to the total applied lateral force) is employed.

In passing, a similar analysis of plates on elastic foundation can be performed using the energy expression obtained by Hui and Hansen (1980b).

3. NON-STATIONARY CREEP RESPONSE

The constitutive power law for uniaxial creep of ice was introduced by Glen (1955) and an extension to include a time hardening exponential function was suggested by Assur (1979). It takes the form

$$\dot{\varepsilon}^c = K|\bar{\sigma}|^n \text{ sign } (\bar{\sigma})g(t) \tag{9a}$$

$$g(t) = [(1/t) \exp (t-1)]^\beta \tag{9b}$$

where $t = \bar{t}/\bar{t}_r$, $\bar{t}$ and $\bar{t}_r$ are time and reference time, respectively, $\dot{(\ )} = \mathrm{d}(\ )/\mathrm{d}t$, $\dot{\varepsilon}^c$ is the creep strain rate, $\bar{\sigma}$ is the axial stress and sign $(\bar{\sigma}) = 1$ for $\bar{\sigma} \geqslant 0$ and sign $(\bar{\sigma}) = -1$ for $\bar{\sigma} \leqslant 0$. Note that time $\bar{t} = 0$ refers to the elastic state just prior to the creep behavior. The time hardening function $g(t)$ is unity for the time hardening exponent being zero. Further, the function $g(t)$ decreases as time increases for $t < 1$ and it increases with time for $t > 1$; the minimum value occurs at $g(t = 1) = 1$. Other viscoplastic constitutive laws are possible (Hui and de Oliveira, 1986) and a thorough discussion on the constitutive laws for ice can be found in the papers by Morland (1979), Christensen (1982), Szyszkowski *et al.* (1985) and Xirouchakis and Wierzbicki (1985), among others.

For a time-independent stress and no time hardening, the above strain rate expression can be integrated to yield

$$\bar{t} = \varepsilon^c/[K|\bar{\sigma}|^n \text{ sign } (\bar{\sigma})]. \tag{10}$$

The reference time may be found by selecting a nominal value of the stress $\bar{\sigma}$ and strain ε^c. Here, $\bar{\sigma}$ is chosen to be the elastic axial stress at the beam center bottom fiber and ε^c is chosen to be the elastic strain at the same location, that is

$$\bar{\sigma} \to \bar{\sigma}_b = |\bar{\sigma}(t = X = 0, Z = H - Z_0)| = |(H - Z_0)(aE_0)W_{,XX}(\bar{t} = X = 0)| \tag{11a}$$

$$\varepsilon^c \to \bar{\sigma}_b/(aE_0) \tag{11b}$$

where aE_0 is Young's modulus at the bottom fiber. Thus, the reference time becomes

$$\bar{t}_r = 1/(aE_0K|\bar{\sigma}_b|^{n-1}). \tag{12}$$

The choice of this reference time is quite arbitrary since one can choose the creep parameter K in the constitutive equation to fit the experimental data. However, this reference time has proven to be advantageous in certain creep buckling problems (Obrecht, 1977).

The above power law can be generalized to multi-axial creep with the aid of Prandtl–Reuss equations of incremental plasticity (Odqvist, 1976; Palmer, 1967)

$$\dot{\varepsilon}^c_{ij} = s_{ij}(3K/2)(\bar{\sigma}_{\text{eff}})^{n-1}g(t). \tag{13}$$

In the above expression, $\dot{\varepsilon}^c_{ij}$ is the creep strain rate and the stress deviator s_{ij} and the effective stress $\bar{\sigma}_{\text{eff}}$ are defined by

$$s_{ij} = \bar{\sigma}_{ij} - (\delta_{ij}/3)(\bar{\sigma}_{11} + \bar{\sigma}_{22} + \bar{\sigma}_{33}) \tag{14}$$

$$(\bar{\sigma}_{\text{eff}})^2 = 3J_2 = (1/2)[(\bar{\sigma}_{11} - \bar{\sigma}_{22})^2 + (\bar{\sigma}_{22} - \bar{\sigma}_{33})^2 + (\bar{\sigma}_{33} - \bar{\sigma}_{11})^2 + 6(\bar{\sigma}^2_{12} + \bar{\sigma}^2_{23} + \bar{\sigma}^2_{13})] \tag{15}$$

where J_2 is the second invariant of the stress deviator and $\delta_{ij} = 1$ for $i = j$ and $\delta_{ij} = 0$ for $i \neq j$ and subscripts 1, 2 and 3 correspond to the X-, Y- and Z-directions, respectively.

The total strain rate can be written as the sum of the elastic and creep components (plastic strain rate is neglected)

$$\dot{\varepsilon}_{ij} = \dot{\varepsilon}^{e}_{ij} + \dot{\varepsilon}^{c}_{ij}. \tag{16}$$

The linear elastic strain rates for an isotropic material are

$$\dot{\varepsilon}^{e}_{ij} = [(1+\nu)(\delta_{ik}\delta_{jl}) - \nu\delta_{ij}\delta_{kl}][\dot{\bar{\sigma}}_{kl}/E(Z)] \tag{17}$$

where ν is Poisson's ratio. Furthermore, for small deflections, the total strain rates $\dot{\varepsilon}_{ij}$ can be expressed in terms of the deflection rates in the form

$$\dot{\varepsilon}_{ij} = -Z\dot{W}_{,ij}. \tag{18}$$

For a beam, $\bar{\sigma}_{22} = \bar{\sigma}_{33} = \bar{\sigma}_{12} = \bar{\sigma}_{13} = \bar{\sigma}_{23} = 0$ so that $\bar{\sigma}_{\text{eff}} = \bar{\sigma}_{11}$ and the elastic strain rate becomes

$$\dot{\varepsilon}^{e}_{ij} = -Z\dot{W}_{,XX} - K|\bar{\sigma}|^{n} \text{ sign } (\bar{\sigma})g(t) \tag{19}$$

and the bending moment rate is defined as ($\dot{M}_{22} = 0$ and $\dot{M}_{12} = 0$)

$$\dot{M}_{11} = \int_{Z=-Z_0}^{H-Z_0} ZE(Z)\dot{\varepsilon}^{e}_{11}\,\mathrm{d}Z = -D_1\dot{W}_{,XX} - Kg(t) \text{ sign } (\bar{\sigma}) \int_{Z=-Z_0}^{H-Z_0} ZE(Z)|\bar{\sigma}|^{n}\,\mathrm{d}Z. \tag{20}$$

Moreover, the governing differential equation for a beam attaching to a liquid elastic foundation is

$$K_1\dot{W} - B\dot{M}_{11,XX} = \dot{P}(X) \tag{21}$$

which can be re-written in the form

$$BD_1\dot{W}_{,XXXX} + K_1\dot{W} = \dot{P}(X) - BKg(t) \text{ sign } (\bar{\sigma}) \int_{Z=-Z_0}^{H-Z_0} (|\bar{\sigma}|^{n})_{,XX} ZE(Z)\,\mathrm{d}Z. \tag{22}$$

Introducing the non-dimensional stress defined by $\sigma = \bar{\sigma}/\bar{\sigma}_b$ and from now on $\dot{(\,)} = \mathrm{d}(\,)/\mathrm{d}t$, one obtains the governing differential equation for the non-stationary creep problem ($t = \bar{t}/\bar{t}_r$, $z = Z/H$)

$$\dot{w}_{,xxxx} + 4\dot{w} = \dot{p}(x) - c_0 \text{ sign } (\sigma) \int_{z=-z_0}^{1-z_0} (|\sigma|^{n})_{,xx} zE(Z)/E_0\,\mathrm{d}z \tag{23a}$$

where

$$c_0 = [12/(ad_1)]g(t)(\bar{\sigma}_b/E_0). \tag{23b}$$

Furthermore, the non-dimensional stress rate can be computed from

$$\dot{\sigma} = [E(Z)/E_0][-z\dot{w}_{,xx}(E_0/\bar{\sigma}_b) - \text{sign } (\sigma)g(t)(|\sigma|^{n}/a)] \tag{24a}$$

where the elastic stress at the beam center bottom fiber is

$$\bar{\sigma}_b/E_0 = |a(1-z_0)w_{,xx}(t = x = 0)|. \tag{24b}$$

The boundary conditions at the beam center are

$$\dot{w}_{,x}(x = 0) = 0 \tag{25a}$$

$$\dot{w}_{,xxx}(x = 0) = (\dot{f}/2) - c_0 \text{ sign } (\sigma) \int_{z=-z_0}^{1-z_0} (|\sigma(x = 0)|^n)_{,x} z E(Z)/E_0 \, dz. \tag{25b}$$

At the beam end, the boundary condition related to zero slope-rate or zero moment-rate conditions is

$$\dot{w}_{,x}(x = L/(2\lambda)) = 0 \tag{26a}$$

or

$$\dot{w}_{,xx}(x = L/(2\lambda)) = -c_0 \text{ sign } (\sigma) \int_{z=-z_0}^{1-z_0} |\sigma(x = L/(2\lambda))|^n z E(Z)/E_0 \, dz \tag{26b}$$

while the one related to the zero deflection-rate or zero shear force-rate condition is

$$\dot{w}(x = L/(2\lambda)) = 0 \tag{27a}$$

or

$$\dot{w}_{,xxx}(x = L/(2\lambda)) = -c_0 \text{ sign } (\sigma) \int_{z=-z_0}^{1-z_0} (|\sigma(x = L/(2\lambda))|^n)_{,x} z E(Z)/E_0 \, dz. \tag{27b}$$

4. NUMERICAL SCHEME

The governing fourth-order differential equation in the deflection rate $\dot{w}$ is discretized using the central finite difference scheme with N (approximately 51) grid points from $x = 0$ to $L/(2\lambda)$, assuming that the loading is symmetric with respect to the beam center. It should be cautioned that the numerical solution of the governing equation is complicated by the fact that as time tends to 0^+, the creep strain rate becomes infinite. In order to deal with this problem, the stress σ (defined to be $\bar{\sigma}/\bar{\sigma}_b$) is taken to remain unchanged from its elastic value at $t = 0$ for a sufficiently small value of the first time step at $t = \Delta t$ (Obrecht, 1977). The integration across the thickness is performed using Simpson's rule with approximately $J_U = 9$ and $J_L = 15$ integration points across the upper (above the neutral axis, $z = -z_0$ to 0) and lower portions of the beam, respectively. The discretized linear non-homogeneous equations are solved using a Gaussian elimination equation solver LINPACK (Dongarra *et al.*, 1979; Hui, 1984). Further, the non-dimensional stress-rate vector, being a function of both the x- and z-coordinates, is computed based on the displacement-rate vector $\dot{w}$ and the stress matrix σ (function of both x and z). Time integration for the deflection and stresses is performed using Euler's integration scheme

$$w(t = t_i) = w(t = t_{i-1}) + (\Delta t)\dot{w}(t = t_{i-1}) \tag{28a}$$

$$\sigma(t = t_i) = \sigma(t = t_{i-1}) + (\Delta t)\dot{\sigma}(t = t_{i-1}) \tag{28b}$$

where t_i is the current time and t_{i-1} is the previous time ($t_i = t_{i-1} + \Delta t$). The above procedure is repeated for the next time increment until the deflection vector $w(t, x)$ reaches the asymptotic value as time tends to infinity or the deflection exceeds the plate thickness. Note that as time tends to infinity, the beam relaxes completely and the load is fully carried by the underlying liquid foundation so that the second derivative of the moment $M_{,xx}$ vanishes.

The above procedure may be quite time consuming since the chosen uniform time step Δt has to be sufficiently small in order that the solution can converge. In most creep

problems, it is desirable to have small time step near $t = 0$ while a relatively coarse time step will suffice for large time. A variable time step was suggested based on the proposition that the incremental effective creep strain should be very much smaller (say $\alpha = 4\%$) than the effective elastic strain (Sutherland, 1970; Shimizu, 1974, Section 6.2). In this case, the time step is given by

$$\Delta t_i = \alpha/[|\sigma(t = t_i, x, z)|^n K g(t = t_i) E(Z)]. \tag{29}$$

The above minimum time step occurs at the beam center top fiber so that one may set $E(Z) = E_0$ and $\sigma(t = t_i, x, z) = \sigma(t = t_i, x = 0, z = -z_0)$. In non-dimensional form, the time step becomes

$$\Delta t_i = (a\alpha)/[g(t = t_i)|\sigma(t = t_i, x = 0, z = -z_0)|^{n-1}] \tag{30}$$

where $\sigma = \bar{\sigma}/\bar{\sigma}_b$ and $\bar{\sigma}_b = |\sigma(t = 0, x = 0, z = 1 - z_0)|$. As a check on the validity of the above time step, the alternative expression is given based on the work presented by Cormeau (1975)

$$\Delta \bar{t}_i \leqslant 4/[(3E_0K)g(t = t_i)n|\bar{\sigma}(\bar{t} = \bar{t}_i, X = 0, Z = -Z_0)|^{n-1}] \tag{31}$$

or in non-dimensional form

$$\Delta t_i \leqslant (4a)/[(3n)g(t = t_i)|\sigma(t = t_i, x = 0, z = -z_0)|^{n-1}]. \tag{32}$$

Since the factor $\alpha = 0.04$ is less than $4/(3n)$ for $n < 33$ (it takes the value 1.33 and 0.444 for $n = 1$ and 3, respectively), it can be seen that the present time step satisfies the stability limit requirement reported by Cormeau.

Since the time hardening exponential function $g(t)$ is infinite at $t = 0$, the value of $g(t = t_1)$ is taken to be unity in the computation of the first time step Δt_1. This assumption is necessary in order to avoid numerical difficulty and the specification of the factor α is required in formulating the numerical solution.

5. ELASTIC SOLUTION OF A BEAM UNDER A SINUSOIDAL LATERAL LOAD

As an example problem, the creep behavior of a simply supported floating ice beam subjected to a sinusoidal load is examined. Among the numerous possible loading configurations, the sinusoidal load is the simplest possible distributed load (Hetenyi, 1946; Flugge, 1975) where the closed form solution for the elastic response can be found. Further, the possibility of "lift-off" between the ice and the liquid foundation is avoided for all times. Of particular interest is the investigation of the effects of variations of the time hardening exponent β and Young's modulus parameters a, b on the non-stationary creep response of floating ice beams.

The applied sinusoidal load as a function of the axial coordinate X (in the shape of a half sine wave) is

$$P(X) = Q \sin [(\pi X/L) + (\pi/2)] \tag{33}$$

or in non-dimensional form

$$p(x) = q \sin [\bar{m}x + (\pi/2)] \tag{34}$$

where $\bar{m} = \pi\lambda/L$ and $q = QH\lambda^2/(D_1 B)$. The total force on the structure can then be computed from

$$\int_{X=-L/2}^{L/2} P(X)\, dX = qK_1\lambda^3/(2\bar{m}H) = 2qLD_1B/(\lambda^2\pi H) = 2QL/\pi. \tag{35}$$

Thus, the elastic deflection and the elastic stress are

$$w(t=0) = [q/(\bar{m}^4+4)] \sin [\bar{m}x+(\pi/2)] \tag{36a}$$

$$\bar{\sigma}(t=0, x, z)/\bar{\sigma}_b = [-zE(Z)/\bar{\sigma}_b]w_{,xx}(t=0) = [zE(Z)/\bar{\sigma}_b]\left(\frac{q\bar{m}^2}{\bar{m}^4+4}\right) \sin [\bar{m}x+(\pi/2)]. \tag{36b}$$

Further, the elastic stress at the beam center bottom fiber is ($x = 0$, $z = 1-z_0$ and note that $E(z = 1-z_0) = aE_0$)

$$\bar{\sigma}_b/E_0 = |a(1-z_0)q\bar{m}^2|/(\bar{m}^4+4) \tag{37}$$

so that by equating $\bar{\sigma}_b$ to the failure stress $\bar{\sigma}_f$, the value of q for instantaneous elastic failure is

$$q_f = \frac{(\bar{m}^4+4)(\bar{\sigma}_f/E_0)}{a(1-z_0)\bar{m}^2}. \tag{38}$$

The above expressions can be re-arranged into the form

$$w(t=0) = \left(\frac{(q/q_f)(\bar{\sigma}_f/E_0)}{a(1-z_0)\bar{m}^2}\right) \sin [\bar{m}x+(\pi/2)] \tag{39}$$

$$\sigma(t=0) = \left(\frac{[zE(Z)/E_0]}{a(1-z_0)}\right) \sin [\bar{m}x+(\pi/2)] \tag{40}$$

$$\bar{\sigma}_b/E_0 = (q/q_f)(\bar{\sigma}_f/E_0). \tag{41}$$

6. DISCUSSION OF RESULTS

The floating ice beam under a sinusoidal load is assumed to possess a linear variation of Young's modulus across the thickness (so that $b = 1$) and the creep exponent is taken to be 3. Due to the large number of parameters involved in this paper, only the following four cases will be examined:

(i) homogeneous short beam ($a = 1$, $L/(\lambda\pi) = 0.2$);
(ii) non-homogeneous short beam ($a = 0.25$, $L/(\lambda\pi) = 0.2$);
(iii) homogeneous long beam ($a = 1$, $L/(\lambda\pi) = 1.0$);
(iv) non-homogeneous long beam ($a = 0.25$, $L/(\lambda\pi) = 1.0$).

It is hoped that these cases represent an unbiased parameter study of the creep problem.

Figure 1(a) shows a graph of central deflection (normalized with respect to its elastic value at the beam center) vs non-dimensional time $\bar{t}/\bar{t}_f$ for a floating homogeneous short beam. The time being considered involved both the primary creep ($\bar{t}/\bar{t}_r < 1$) and the tertiary creep ($\bar{t}/\bar{t}_r > 1$) ranges. It can be seen that as the time hardening exponent β is increased, the deflections also increase. For sufficiently large time, the beam relaxes completely and the load is fully carried by the elastic foundation. The asymptotic value of the deflection for large time can be obtained from

$$\frac{w(t\to\infty, x=0)}{w(t=x=0)} = \frac{q/4}{w(t=x=0)} = 1+(\bar{m}^4/4). \tag{42}$$

Further, the value of the load intensity q has no effect on the present non-dimensional deflections since the factor q cancels out when one divides the deflection by its initial ($t = 0$) value.

Figure 1(b) shows a plot of the axial stress at the beam center extreme fiber (again normalized with respect to its elastic value) vs $\bar{t}/\bar{t}_r$ for a floating homogeneous short beam. As the time hardening exponent β increases from 0 to 1.0, the axial stresses further relax. Further, the stress rate decreases with time in the primary creep range and increases with time in the tertiary creep regime. Again, the value of q has no effect on these curves. Figure 1(c) shows the stress profiles across the beam thickness at the beam center of a homogeneous short beam for various values of $\bar{t}/\bar{t}_r$ with no time hardening. Note that the stress profile is linear at $t = 0$ and it relaxes with time.

In order to estimate the failure time based on a given value of the applied load q/q_f, it

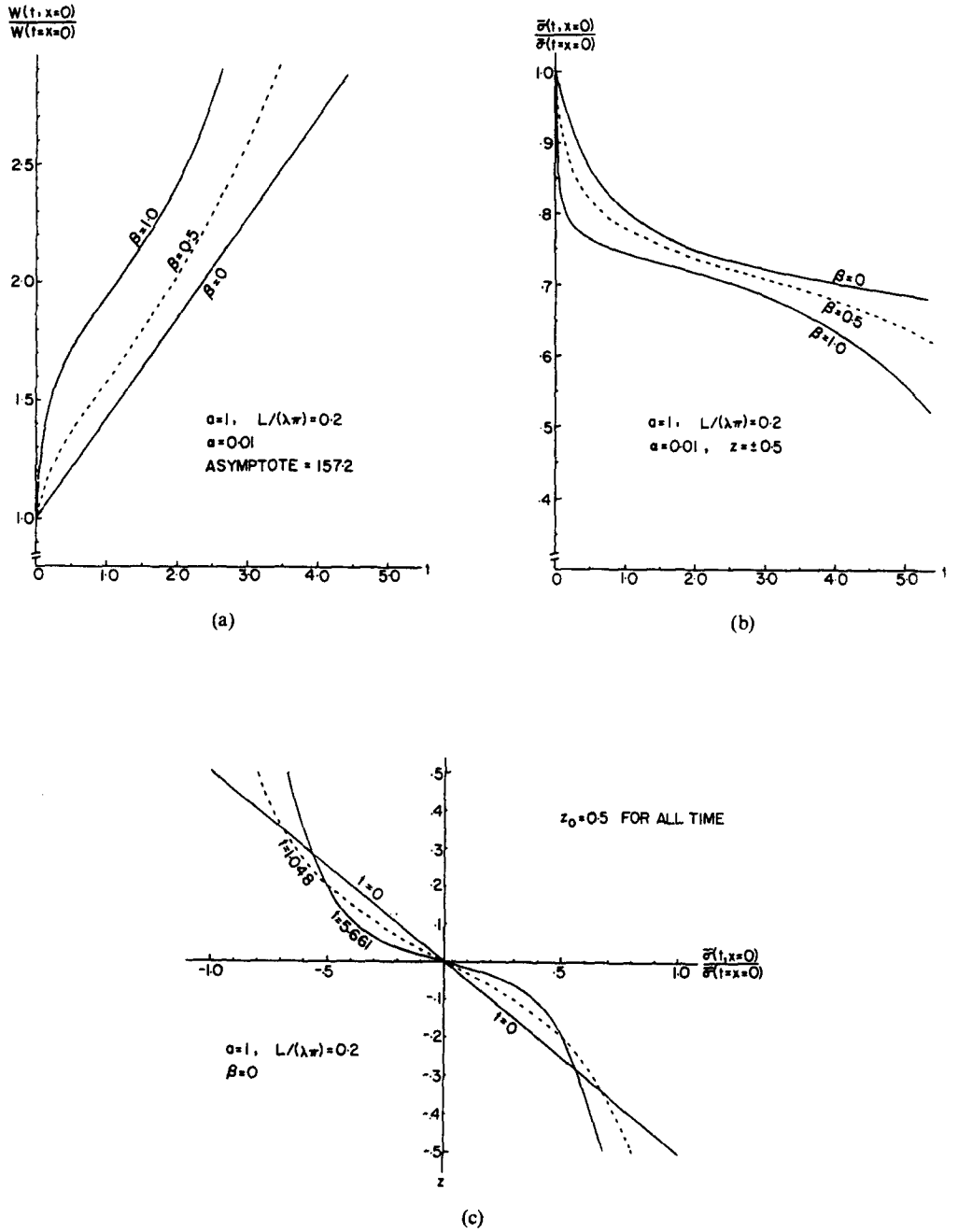

Fig. 1. (a) Normalized deflection vs non-dimensional time for floating homogeneous short beams. (b) Normalized stress vs non-dimensional time for floating homogeneous short beams. (c) Normalized stress profile at the beam center for floating homogeneous short beams.

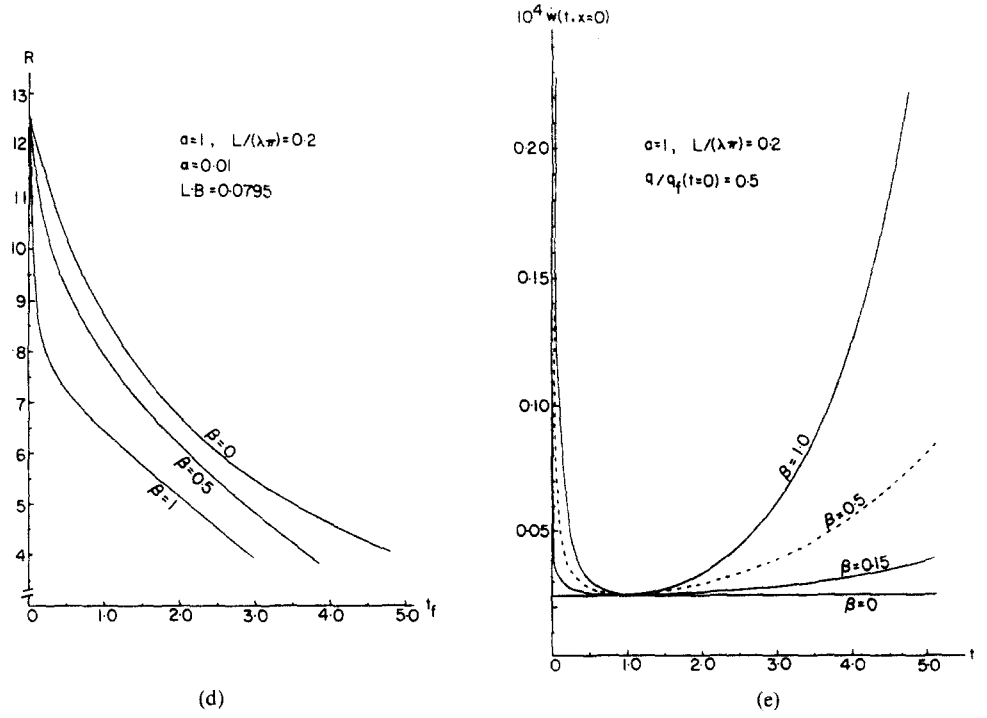

(d) (e)

Fig. 1. (d) Load factor R vs failure time for floating non-homogeneous short beams. (e) Initial deflection rate vs non-dimensional time for floating homogeneous short beams.

is desirable to rearrange eqn (39) into the form

$$\frac{w(t=t_f,\, x=0)}{w(t=0,\, x=0)} = \frac{a(1-z_0)\bar{m}^2 w(t=t_f,\, x=0)}{(q/q_f)(\bar{\sigma}_f/E_0)} \tag{43}$$

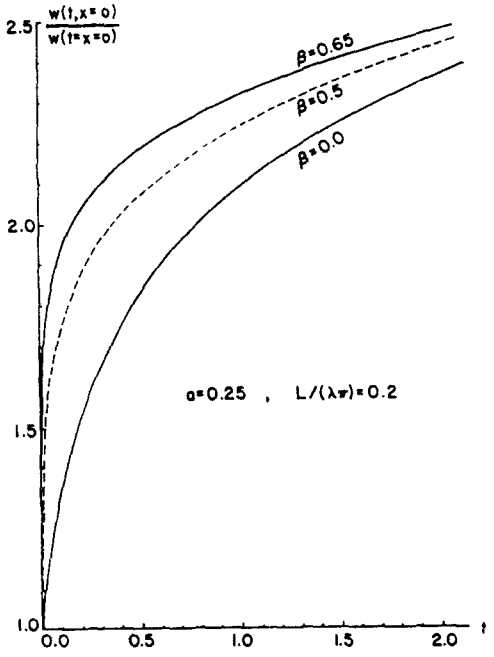

Fig. 2(a). Normalized deflection vs non-dimensional time for floating non-homogeneous short beams.

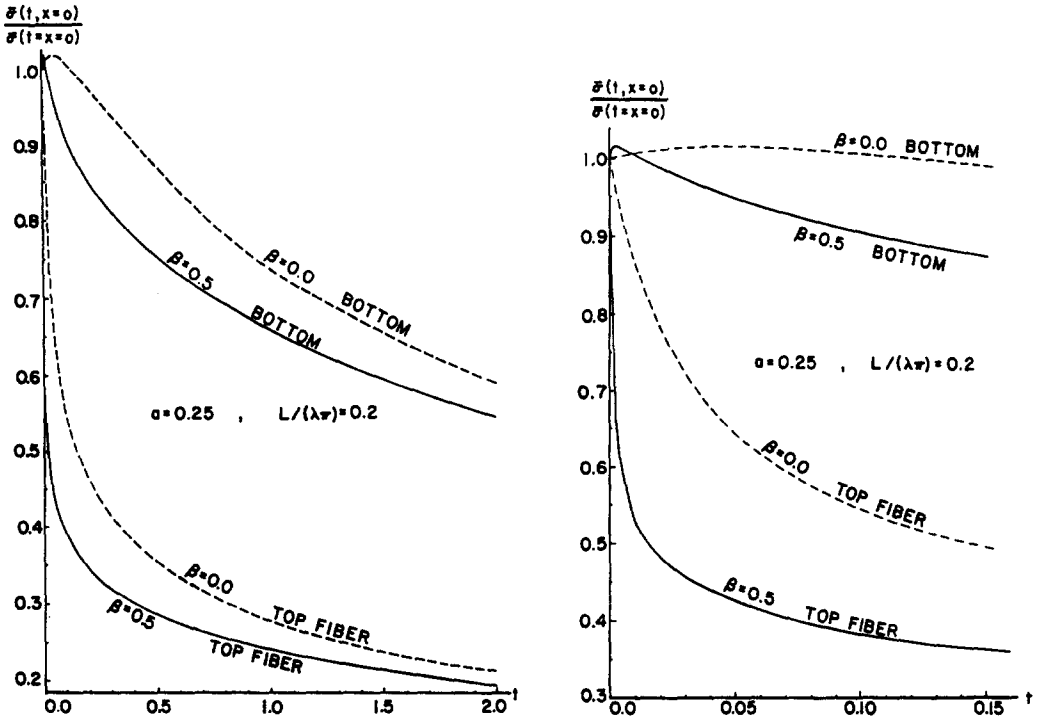

Fig. 2(b) (i) and (ii). Normalized stress vs non-dimensional time for floating non-homogeneous short beams.

so that the load factor R may be plotted against the failure time t_f where

$$R \triangleq \frac{(q/q_f)(\bar{\sigma}_f/E_0)}{w(t=t_f,\, x=0)} = \frac{(a)(1-z_0)\bar{m}^2}{[w(t=t_f,\, x=0)/w(t=x=0)]}. \tag{44}$$

Figures 1(d) and 2(d) show that as the time hardening parameter β increases for a fixed value of the load factor R, the failure time decreases. Since there exist upper bounds for

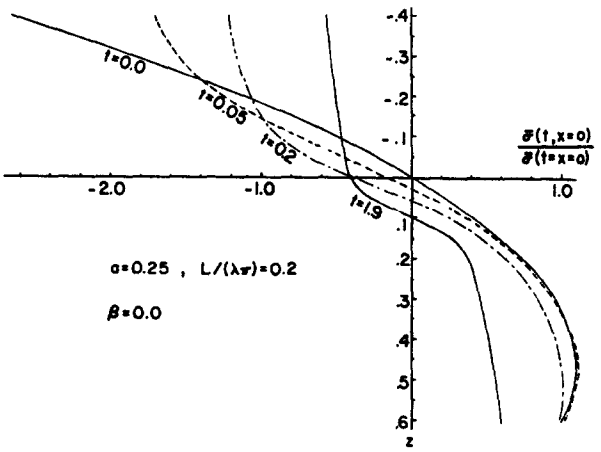

Fig. 2(c). Normalized stress profile at the beam center for floating non-homogeneous short beams.

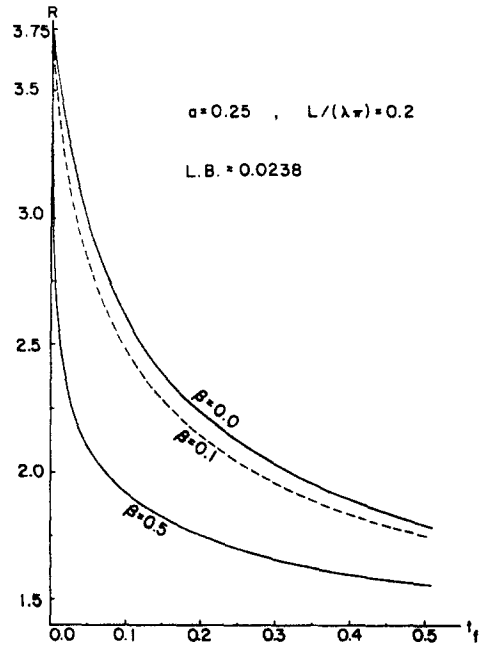

Fig. 2(d). Load factor R vs failure time for floating non-homogeneous short beams.

the deflections, all these curves will asymptote to certain lower bounds (as specified in the figures)

$$\text{L.B.} = \frac{(a)(1-z_0)\bar{m}^2}{1+(\bar{m}^4/4)}. \tag{45}$$

As expected, Fig. 1(e) shows that the strain rate and hence the deflection rate decreases with time in the primary creep range whereas it increases with time in the tertiary creep regime for a homogeneous short beam. The deflection rate increases significantly as time tends to infinity or time tends to zero for $\beta = 1.0$. The effects are less pronounced for $\beta = 0.15$ and 0.5.

For a non-homogeneous short beam ($a = 0.25$, $L/(\lambda\pi) = 0.2$), Fig. 2(a) shows that the above observations are still qualitatively valid in the time range $\bar{t}/\bar{t}_r \leqslant 2.0$ being considered. Unlike the homogeneous beam, Fig. 2(b) (i) shows that the stresses at the beam center top fiber are found to relax with time much more rapidly than the bottom fiber. In fact, the stresses at the bottom fiber for a non-homogeneous short beam actually increase slightly with time initially and then decrease with time. A magnified view of these curves for a shorter time range is presented in Fig. 2(b) (ii).

Judging from the stress profile across the beam center thickness, Fig. 2(c) shows that in the absence of time hardening ($\beta = 0$), it is evident that the stresses do not necessarily relax with time near the bottom portion of the ice beam. Further, it should be emphasized that the stationary creep solution is not assumed in the present study. Indeed, since the ratios of the stress between the top and bottom fibers at the beam center for various times are not constant, the creep solutions for non-homogeneous beams (Fig. 2(c)) are not stationary even though they are stationary for homogeneous beams (Fig. 1(c)). For non-homogeneous short beams, the top fiber relaxes much more with time than the bottom fiber.

In order to assess the initial deformation and stress behavior in the vicinity of $t = 0$, the deflection rate and the stress rate at $t = 0$ are obtained in the following closed form (see the Appendix)

$$\frac{\dot{w}(t=0, x=0)}{w(t=0, x=0)} = \left(\frac{3}{\bar{m}^4+4} + \frac{9}{81\bar{m}^4+4}\right)\left(\frac{3\bar{m}^4 A_3}{d_1 a^3(1-z_0)^2}\right) \tag{46}$$

$$\dot{\sigma}(t=0,\ x=0,\ z)=\left(\frac{zE(Z)/E_0}{a^4(1-z_0)^3}\right)\left\{\left(\frac{3}{\bar{m}^4+4}+\frac{81}{81\bar{m}^4+4}\right)\left(\frac{3A_3\bar{m}^4}{d_1}\right)-z^2[E(Z)/E_0]^3\right\} \tag{47}$$

where

$$A_3=\int_{-z_0}^{1-z_0}[zE(Z)/E_0]^4\,dz. \tag{48}$$

The deflection rate and the stress rate at the beam center at $t=0$ vs $L/(\lambda\pi)$ for homogeneous and non-homogeneous beams are shown in Figs 3(a)–(c). It can be seen that the magnitude of the initial deflection rate at the beam center as well as the magnitude of the initial stress rate (at beam center top and bottom fibers) are much higher in the non-homogeneous beam than those in a homogeneous beam. Note that the axial stress is positive (tension) below the neutral axis and negative (compression) above it. Thus, of particular interest is the fact that the initial stress rate at the beam center bottom fiber for a non-homogeneous beam (except for a very long beam where $L/(\lambda\pi)>2.5$ in which it asymptotes to -1.0) is positive which indicates that the magnitude of the stress increases with time at least for sufficiently small time.

Finally, the typical stress profile at the beam center (normalized with respect to its elastic value at the beam center bottom fiber) for a floating homogeneous long beam is shown in Fig. 4(a). Comparing the stress profiles between homogeneous long and short beams (Figs 4(a) and 1(c)), the axial stress near the neutral axis does not change significantly with time for a long beam whereas it changes for a short beam.

The stress profiles of a non-homogeneous long beam at the beam center (Fig. 4(b)) and a non-homogeneous short beam (Fig. 2(c)) have different trends. The maximum tensile and maximum compressive stresses decrease in magnitude with time for a non-homogeneous long beam. On the other hand, for a non-homogeneous short beam (Fig. 2(c)), the maximum tensile stress (below the neutral axis) increases slightly with time initially and then decreases

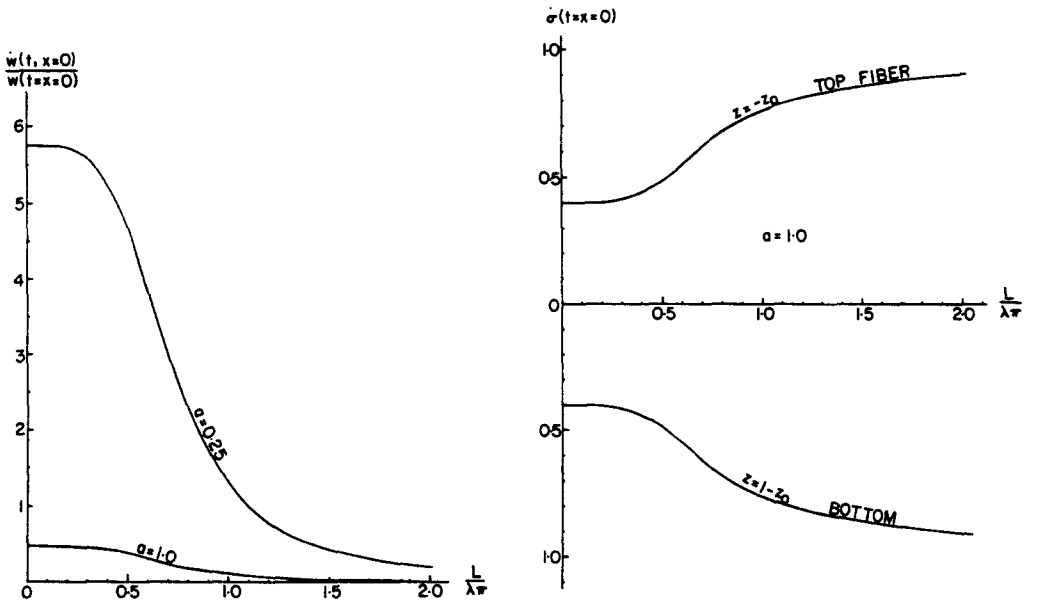

(a) (b)

Fig. 3. (a) Initial deflection rate vs non-dimensional length parameter for $a=0.25$ and 1. (b) Initial stress rate vs non-dimensional length parameter for floating homogeneous beams ($a=1$, $x=0$, $t=0$).

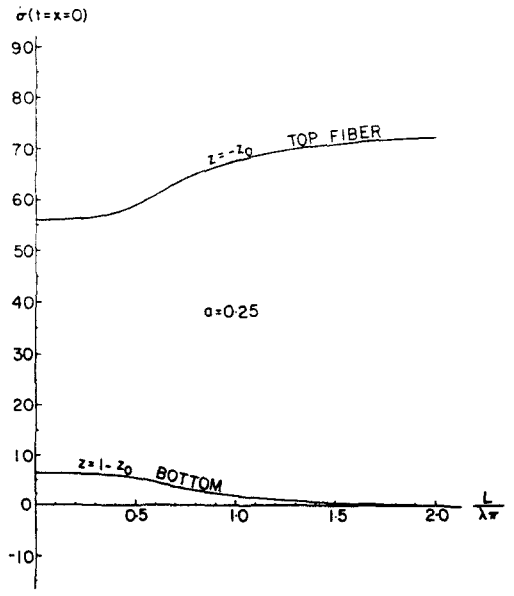

Fig. 3(c). Initial stress rate vs non-dimensional length parameter for floating non-homogeneous beams ($a = 0.25$, $x = 0$, $t = 0$).

subsequently and the maximum compressive stress (above the neutral axis) decreases with time. Thus, the stress relaxation behavior is quite different between long and short beams.

Figure 5(a) depicts a graph of the shift of the neutral axis at the beam center vs $\bar{t}/\bar{t}_r$ for non-homogeneous long and short beams with no time hardening. Note that the neutral axis does not change with time for a homogeneous beam. The neutral axis tends to shift from $z_0 = 0.4$ (based on a linear variation of Young's modulus with $a = 0.25$) at $t = 0$ to a value close to 0.5. The short beam is more sensitive to the shift in the neutral axis with time than the long beam.

Finally, typical shifts of the location of the neutral axis as a function of the axial coordinate for various values of $\bar{t}/\bar{t}_r$ are shown in Fig. 5(b). It can be seen that for a large value of the axial coordinate (where the lateral load is much smaller than at the beam center) the axial stresses are smaller than that at the beam center and the neutral axis remains approximately unchanged at $z_0 = -0.4$.

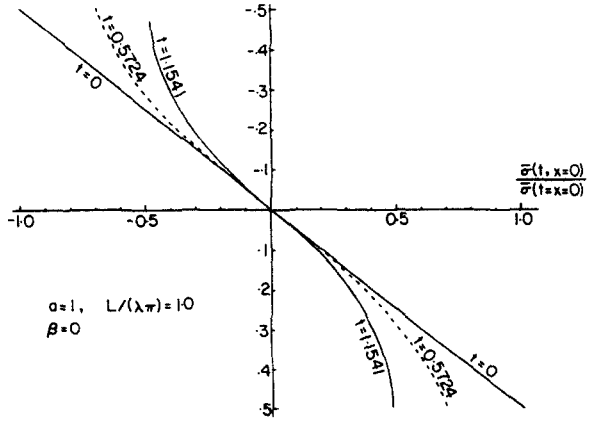

Fig. 4(a). Normalized stress profile at the beam center for floating homogeneous long beams.

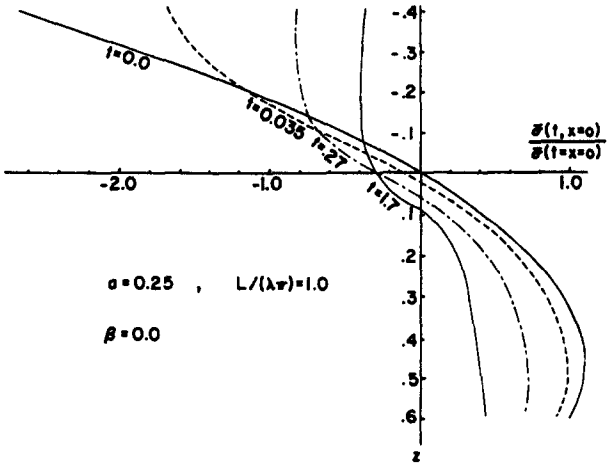

Fig. 4(b). Normalized stress profile at the beam center for floating homogeneous long beams.

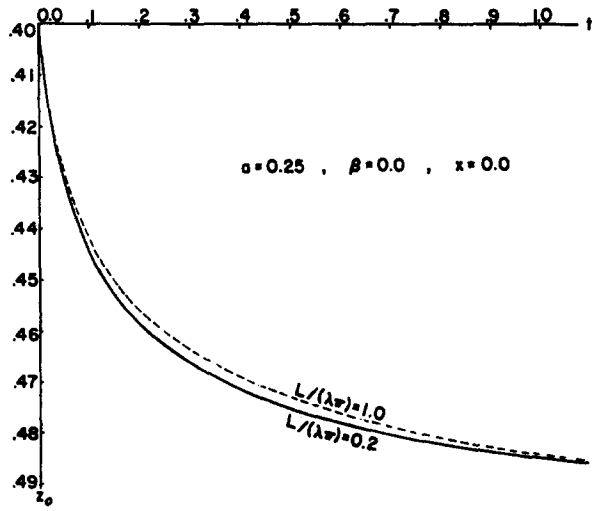

Fig. 5(a). Location of the neutral axis vs the axial coordinate for various non-dimensional time.

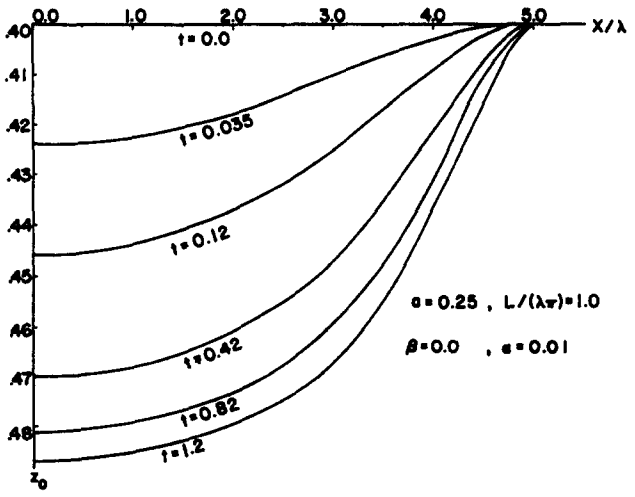

Fig. 5(b). Location of the neutral axis at the beam center vs non-dimensional time for non-homogeneous long and short beams (neutral axis is independent of time for homogeneous beams).

7. CONCLUDING REMARKS

The non-linear creep behavior of floating ice beams is examined. It is found that the effect of time hardening in the power-type constitutive relation is to increase the deflection and further relax the stresses. The strain rate (and hence the deflection rate and the stress rate) decreases with time in the primary creep range ($\bar{t}/\bar{t}_r < 1$) whereas it increases with time in the tertiary creep regime ($\bar{t}/\bar{t}_r > 1$). While the trends in the deflections between the homogeneous and non-homogeneous beams are qualitatively similar, the stresses and stress profile display a significantly different trend. In fact, the stresses do not necessarily relax with time initially for a non-homogeneous beam. The neutral axis is found to change with time for a non-homogeneous beam and it is independent of time for a homogeneous beam.

Acknowledgements—This research work was financially supported by the National Science Foundation (initiation grant under contract with the Massachusetts Institute of Technology) and by the National Oceanic and Atmospheric Administration through the Ohio Sea Grant Program (Grant No. 716576). The work was also supported by the Ohio State University Seed Grant through the Office of Research and Graduate Studies. The first author would like to thank Dr Andrew Assur for an interesting discussion at CRREL on the time hardening constitutive equation for ice.

REFERENCES

Assur, A. (1979). Some promising trends in ice mechanics. *Physics and Mechanics of Ice, IUTAM Symposium* (Edited by P. Tryde), August, pp. 1–15.

Carstens, T. (Editor) (1984). Int. Association for Hydraulic Research, Seventh IAHR Symposium on Ice, Hamburg, West Germany, 27–31 August.

Chen, V. L., Chen, E. S. and Vivatrat, V. (1985). Constitutive modeling of sea ice. Seventeenth Annual Offshore Technology Conf. (OTC), 6–9 May, pp. 343–351.

Christensen, R. M. (1982). *Theory of Viscoelasticity*, 2nd Edn. Academic Press, New York.

Cormeau, I. (1975). Numerical stability in quasi-static elasto/visco-plasticity. *Int. J. Numer. Meth. Engng* **9**, 100–127.

Dongarra, J., Moler, C. B., Bunch, J. R. and Stewart, G. W. (1979). LINPACK Users' Guide. Society for Industrial and Applied Mathematics, Philadelphia.

Duval, P., Maitre, M., Manouvrier, A., Marec, G. and Jay, J. C. (1981). Primary creep and experimental method for testing ice in various conditions of strain rates and stresses. IAHR Int. Symposium on Ice, Quebec City, Canada, pp. 433–439.

Findley, W. N., Lai, J. S. and Onaran, K. (1976). Creep and relaxation of nonlinear viscoelastic materials. *North-Holland Series in Applied Mathematics and Mechanics* (Edited by H. A. Lauwerier and W. T. Koiter), Vol. 18.

Findley, W. N., Poczatek, J. J. and Mathur, P. N. (1958). Prediction of creep in bending from tension- and compression-creep data when creep coefficients are unequal. *Trans. ASME* **80**(6), 1294–1298.

Flugge, W. (1975). *Viscoelasticity*, 2nd Edn. Springer, Berlin.

Fransson, L. (1985). Load bearing capacity of an ice cover subjected to concentrated loads. ASME Fourth Int. Offshore Mechanics and Arctic Engineering Symposium, Dallas, Texas (Edited by J. Chung *et al.*), pp. 170–176.

Frederking, F. M. W. and Gold, L. W. (1976). The bearing capacity of ice covers under static loads. *Can. J. Civil Engng* **3**(2), 519–538.

Glen, J. W. (1955). The creep of polycrystalline ice. *Proc. R. Soc. London* **A228**(1175), 519–538.

Hamza, H. (1981). Creep failure and fracture of ice. Ph.D. thesis, Faculty of Engng and Applied Science, Memorial University of Newfoundland, St. John's Newfoundland, Canada.

Hamza, H. and Muggeridge, D. B. (1982). Plastic creep bending analysis of plates. *ASCE J. Engng Mech. Div.* **108**(EM6), 1252–1261.

Hetenyi, M. (1946). *Beams on Elastic Foundation*. University of Michigan Press.

Hui, D. and Hansen, J. S. (1980a). The swallowtail and butterfly cuspoids and their application in the initial post-buckling of single-mode structural systems. *Q. Appl. Math.* **38**(1), 17–36.

Hui, D. and Hansen, J. S. (1980b). Two-mode buckling of an elastically supported plate and its relation to catastrophe theory. *ASME J. Appl. Mech.* **47**(3), 607–612.

Hui, D. (1984). Effects of mode interaction on collapse of short, imperfect thin-walled columns. *ASME J. Appl. Mech.* **51**(3), 566–573.

Hui, D. (1985). Viscoelastic analysis of floating non-homogeneous ice sheets under lateral loads. *Proc. of the Tenth Canadian Congress of Applied Mechanics (CANCAM '85)*, London, Ontario, Canada, 2–7 June, pp. E41–E42.

Hui, D. (1986a). Imperfection-sensitivity of elastically supported beams and its relation to the double-cusp instability model. *Proc. R. Soc. London* **A405**, 143–158.

Hui, D. (1986b). Viscoelastic response of floating ice plates under distributed or concentrated loads. *J. Strain Analysis Engng Des.* **21**(3), 135–143.

Hui, D. and de Oliveira, J. G. (1986). Dynamic plastic analysis of impulsively loaded viscoplastic rectangular plates with finite deflections. *ASME J. Appl. Mech.* **53**(3), 667–674.

Jumppanen, P. (Editor) (1983). The Seventh Int. Conf. on Port and Ocean Engineering under Arctic Conditions (POAC). Technical Research Center of Finland, Helsinki, Finland, 5–9 April.

Kerr, A. D. and Palmer, W. T. (1972). The deformations and stresses in floating ice plates. *Acta Mech.* **15**, 57–72.

Kerr, A. D. (1976). The bearing capacity of floating ice plates subjected to static or quasi-static loads. *J. Glaciology* **17**(76), 229–268.
Lainey, L. (1981). Etude Parametrique des Proprietes Mecaniques de la Glace der Mer Resultats D'essais (Parametric study of the mechanical properties of sea ice). Ecole Polytechnique de Montreal, Canada, Centre d'ingenierie Nordique, CINEP Report, 160 pp.
Lunardini, V. J. (1984). *Proc. of the Third Int. Offshore Mechanics and Arctic Engineering (ASME-OMAE) Symposium*, New Orleans, Louisiana, 12–17 February.
Masterson, D. M. and Strandberg, A. G. (1979). Creep and relaxation in floating ice platforms—an analysis of case histories. *Physics and Mechanics of Ice. IUTAM Symposium* (Edited by P. Tryde), August, pp. 205–216.
Mellor, M. (1983). Mechanical behavior of sea ice. Cold Regions Research and Engineering Laboratory. Hanover, N. H., Monograph 83-1, 105 pp.
Mellor, M. and Cole, D. M. (1982). Deformation and failure of ice under constant stress or constant strain-rate. *Cold Regions Sci. Technol.* **5**, 201–219.
Michel, B. (1978). *Ice Mechanics*. Laval University Press, available from Pvaillon Pouliot-Cité Universitaire, C.P. 2447, Quebec, Canada G1K 7R4.
Mohaghegh, M. (1972). Plastic analysis of Coulomb plates and its application to the bearing capacity of sea ice. Ph.D. thesis, University of Washington, April.
Morland, L. W. (1979). Constitutive laws for ice. *Cold Regions Sci. Technol.* **1**, 101–108.
Murat, J. R. (1978a). Essais en Flexion de Plaques de Glace de Mer (Bending of sea ice plates). Ecole Polytechnique de Montreal, Canada, Report EP-78-R-17, 88 pp.
Murat, J. R. (1978b). La Capacite Portante de la Glace de Mer (The bearing capacity of sea ice). Ecole Polytechnique de Montreal, Canada, Report EP-89-R-49, 434 pp.
Murat, J. R. and Degrange, G. (1983). Analysis of the primary flexural creep of sea-ice. Seventh Int. Conf. on Port and Ocean Engng under Arctic Conditions (POAC '83), 5–9 April, Helsinki, Finland, pp. 200–211.
Nevel, D. E. (1976). Creep theory for a floating ice sheet. Cold Regions Research and Engineering Laboratory, CRREL Special Report 76-4, 98 pp., also, Ph.D. thesis, Thayer School of Engineering, Dartmouth College, Hanover, New Hampshire.
Obrecht, H. (1977). Creep buckling and post-buckling of circular cylindrical shells under axial compression. *Int. J. Solids Structures* **13**, 337–355 (1977); also Ph.D. thesis, Div. of Engng and Applied Physics, Harvard University, Nov. 1975, 84 pp.
Odqvist, F. K. G. (1976). *Mathematical Theory of Creep and Creep Rupture*, 2nd Edn. Clarendon Press, Oxford.
Palmer, A. C. (1967). Creep-velocity bounds and glacier-flow problems. *J. Glaciology* **6**(46), 479–488.
Palmer, W. T. (1971). On the analysis of floating ice plates. Ph.D. thesis, New York University, School of Engng and Science (available from University Microfilm).
Panfilov, D. F. (1960). Experimental investigation of the carrying capacity of a floating ice plate. *Isvestia Vsesojuznogo Nauchno-Issledovatelsskogo Instituta Gidratekhniki*, Vol. 64, in Russian.
Ponter, A. R. S., Palmer, A. C., Goodman, D. J., Ashby, M. F., Evans, A. G. and Hutchinson, J. W. (1983). The force exerted by a moving ice sheet on an offshore structure, Part 1. The creep mode. *Cold Regions Sci. Technol.* **8**, 109–118.
Shimizu, T. (1974). Axisymmetric creep analysis by assumed stress hybrid finite element method. Master of Science Thesis, Department of Aeronautics and Astronautics, M.I.T., Sept. 1974 (advisor: Dr T. H. H. Pian).
Sutherland, W. H. (1970). AXICRP—finite element computer code for creep analysis of plane stress, plane strain and axisymmetric bodies. *Nucl. Engng Des.* **11**, 269–285.
Swamidas, A. S. J., El-Tahan, H. and Reddy, D. V. (1978). Viscoelastic finite-element analysis of floating ice islands. National Research Council Workshop on the Bearing Capacity of Ice Covers, 16–17 October, Winnipeg, pp. 1–25.
Szyszkowski, W., Dost, S. and Glockner, P. G. (1985). A nonlinear constitutive model for ice. *Int. J. Solids Structures* **21**, 307–321.
Tinawi, R. and Murat, J. R. (1978). Sea ice—flexural creep. *Proc. of Int. Association of Hydraulic Research (IAHR), Symposium on Ice Problems*, Sweden, August, pp. 49–75.
Tinawi, R. and Gagnon, L. (1984). Behaviour of sea ice plates under long term loading. Seventh Int. Symposium on Ice, Int. Ass. for Hydraulic Research (IAHR), 27–31 August, pp. 103–112.
Vaudray, K. D. and Katona, M. G. (1975). An elastic structural analysis of floating ice sheets by the finite element method, 3rd Int. Conference on Port and Ocean Engineering under Arctic Condition (POAC), August, pp. 439–453.
Vaudray, K. D. (1977). Ice engineering—study of related properties of floating sea-ice sheets and summary of elastic viscoelastic analysis. Civil Engineering Lab., Naval Construction Battalion Centre, Port Hueneme, California, Technical Report R-860, Dec., 81 pp.
Wang, Y. S. (1983). A rate-dependent stress–strain relationship for sea ice. *ASME J. Energy Resour. Technol.* **105**, 2–5.
Weeks, W. F. and Assur, A. (1966). The mechanical properties of sea ice. In *Ice Pressures Against Structures, Proc. Conf. Laval University*, Quebec, 10–11 Nov. National Research Council of Canada Technical Memorandum No. 92, compiled by L. W. Gold and G. P. Williams, pp. 25–78; also U.S. Army CRREL Report II-C3, Sept. 1967.
Xirouchakis, P. C. (1983). The creep behavior of a floating beam. *J. Ship Res.* **27**(4), 271–280.
Xirouchakis, P. C. and Wierzbicki, T. (1985). Uniaxial constitutive equation of ice from beam tests. *ASME J. Energy Resour. Technol.* **107**, 511–515.

APPENDIX: DEFLECTION RATE AND STRESS RATE AT $t = 0$ FOR A SINUSOIDALLY LOADED BEAM

This section aims to obtain analytically the deflection and stress rates at $t = 0$ for a non-homogeneous floating ice beam subjected to a sinusoidally distributed load. A linear variation of Young's modulus profile is assumed.

In order to avoid analytical complications, the creep exponent n is restricted to the value 3 and the load rate is set to zero.

The governing differential equation for the deflection rate is (for n odd, sign $(\sigma) = 1$ and the absolute value sign on the stress can then be removed)

$$\dot{w}_{,xxxx} + 4\dot{w} = c_0 \int_{-z_0}^{1-z_0} (\sigma^n)_{,xx}(z) E(Z)/E_0 \, dz \tag{A1}$$

where

$$c_0 = \frac{12(\bar{\sigma}_b/E_0)}{ad_1} \tag{A2}$$

$$g(t=0) = 1. \tag{A3}$$

The elastic deflection and the elastic stress are

$$w(t=0) = [q/(\bar{m}^4+4)] \sin [\bar{m}x + (\pi/2)] \tag{A4a}$$

$$\sigma(t=0, x, z) = \bar{\sigma}(t=0, x, z)/\bar{\sigma}_b = \left(\frac{[zE(Z)/\bar{\sigma}_b]q\bar{m}^2}{\bar{m}^4+4}\right) \sin [\bar{m}x + (\pi/2)] \tag{A4b}$$

where $\bar{\sigma}_b = (aE_0)(1-z_0)(q\bar{m}^2)/(\bar{m}^4+4)$. Substituting the elastic stress into the above differential equation, one obtains

$$\dot{w}_{,xxxx} + 4\dot{w} = \left(\frac{(-12A_n)(\sigma_b/E_0)}{d_1 a^{n+1}(1-z_0)^n}\right)\{[\sin (\bar{m}x + (\pi/2))]^n\}_{,xx} \tag{A5}$$

where

$$A_n = \int_{-z_0}^{1-z_0} [zE(Z)/E_0]^{n+1} \, dz$$
$$A_3 = A^4 C_4 + 4A^3(a-1)C_5 + 6A^2(a-1)^2 C_6 + 4A(a-1)^3 C_7 + (a-1)^4 C_8 \tag{A6}$$

and the constants C_4, C_5, C_6, C_7, C_8 and A are defined by

$$C_i = \int_{-z_0}^{1-z_0} z^i \, dz, \qquad A = 1 + (a-1)z_0. \tag{A7}$$

Creep exponent $n = 3$

Using the trigonometric identity

$$\sin^3 [\bar{m}x + (\pi/2)] = (3/4) \sin [\bar{m}x + (\pi/2)] - (1/4) \sin [3\bar{m}x + (3\pi/2)] \tag{A8}$$

the differential equation becomes

$$w_{,xxxx} + 4w = (B_0)\{-3 \sin [\bar{m}x + (\pi/2)] + 9 \sin [3\bar{m}x + (3\pi/2)]\} \tag{A9}$$

where

$$B_0 = \frac{(-3A_3\bar{m}^2)(\bar{\sigma}_b/E_0)}{d_1 a^4 (1-z_0)^3}. \tag{A10}$$

The solution which satisfies the boundary conditions is of the form

$$\dot{w}(t=0) = B_1 \sin [\bar{m}x + (\pi/2)] + B_2 \sin [3\bar{m}x + (3\pi/2)]. \tag{A11}$$

Substituting the assumed form of the solution into the differential equation, one obtains

$$B_1 = (-3B_0)/(\bar{m}^4+4)$$
$$B_2 = (9B_0)/(81\bar{m}^4+4). \tag{A12}$$

Thus, the deflection rate at $t = 0$, $x = 0$ is

$$\frac{\dot{w}(t=0, x=0)}{w(t=0, x=0)} = \frac{B_1 - B_2}{w(t=0, x=0)} = \left(\frac{3}{\bar{m}^4+4} + \frac{9}{81\bar{m}^4+4}\right)\left(\frac{3\bar{m}^4 A_3}{d_1 a^3 (1-z_0)^2}\right). \tag{A13}$$

In order to obtain the stress rate at $t = 0$, the above deflection rate is substituted into the stress rate expression

$$\dot{\sigma}(t=0) = \dot{\bar{\sigma}}(t=0)/\bar{\sigma}_b = [E(Z)/E_0]\{-z(E_0/\bar{\sigma}_b)\dot{w}_{,xx}(t=0) - [\sigma(t=0)^3/a]\} \tag{A14}$$

so that (upon evaluating at the beam center $x = 0$)

$$\dot{\sigma}(t = 0,\ x = 0,\ z) = \left(\frac{zE(Z)/E_0}{a^4(1-z_0)^3}\right)\left\{\left(\frac{3}{\bar{m}^4+4} + \frac{81}{81\bar{m}^4+4}\right)\left(\frac{3A_3\bar{m}^4}{d_1}\right) - z^2[E(Z)/E_0]^3\right\}. \tag{A15}$$

The deflection rate and the stress rate at $t = 0$ for the two different beams considered in the present study are summarized in Table A1 (note that $A_3 = 0.0125$ for the homogeneous beam and $A_3 = 0.001907$ for the non-homogeneous beam).

Table A1

	Homogeneous short	Non-homogeneous short	Homogeneous long	Non-homogeneous long
$\frac{\dot{w}(t = 0,\ x = 0)}{w(t = 0,\ x = 0)}$	0.46380	5.7190	0.10588	1.3056
$\dot{\sigma}(t = 0,\ x = 0,\ z = -z_0)$ top fiber	0.40287	56.217	0.76706	68.192
$\dot{\sigma}(t = 0,\ x = 0,\ z = 1-z_0)$ bottom fiber	−0.40287	6.3629	−0.76706	1.8723